 doi:10.20944/preprints202103.0098.v1

Article

Metabolic, organoleptic and transcriptomic impact of *Saccharomyces cerevisiae* genes involved in the biosynthesis of linear and substituted esters.

Philippe Marullo[1,2*#] , Marine Trujillo[1,3#], Rémy Viannais[1], Lucas Hercman[1], Sabine Guillaumie[4], Benoit Colonna-Ceccaldi[3], Warren Albertin[1] and Jean-Christophe Barbe[1*]

[1] Univ. Bordeaux, ISVV, Unité de Recherche Œnologie EA 4577, USC 1366 INRA, Bordeaux INP, F-33140 Villenave d'Ornon, France.
[2] Biolaffort, 11 Rue Aristide Bergès, F-33270 Floirac, France.
[3] Pernod Ricard, 51 Chemin des Mèches, F-94000 Créteil, France.
[4] Univ. Bordeaux, ISVV, UMR 1287 Ecophysiologie et Génomique Fonctionnelle de la Vigne, 210 Chemin de Leysotte, F-33140 Villenave d'Ornon, France.
# Authors contributed equally to this work
* Correspondence: PM philippe.marullo@u-bordeaux.fr; JCB jean-christophe.barbe@agro-bordeaux.fr

Abstract: Esters constitute a wide family of volatile compounds impacting the organoleptic properties of many beverages including wine and beer. They can be classified according to their chemical structure. Higher Alcohols Acetate differ from Fatty Acids Ethyl Esters whereas a third group, Substituted Ethyl Esters, contributes to the fruitiness of red wines. Derived from yeast metabolism, the biosynthesis of Higher Alcohols Acetates and Fatty Acids Ethyl Esters has been widely investigated at the enzymatic and genetic level. In this work, we confirmed their effective contribution in the fruity perception in young red wines by evaluating the effect of their depletion by chemical and sensorial analyses. As previously reported, two pairs of esterases respectively encoded by the paralogue genes (*ATF1*, *ATF2)* and (*EEB1* and *EHT1*) are mostly involved in the biosynthesis of Acetate of Higher alcohols and Fatty Acids Ethyl Esters. However, those esterases have a moderate effect on the biosynthesis of Substituted Ethyl Esters that depends to another pair of genes, *MGL2* and *YJU3* encoding for mono-acyl lipases. These new findings complete our understanding of esters metabolism in the context of wine alcoholic fermentation. In order to evaluate the sensorial impact of esters we attempted to produce a red wine without esters by generating a multiple deletion strain. Surprisingly, we failed to abolish all the esterase activities revealing unsuspected physiological consequences of ester biosynthesis routes. A preliminary RNA-seq analysis depicted the overall impact of the multiple deletion of *ATF1*, *ATF2*, *EEB1* and *EHT1* that triggers the expression shift of 1124 genes involved in nitrogen and lipid metabolism but also chromatin organization and histone acetylation, suggesting an unsuspected regulatory role of ester metabolism.

Keywords: substituted esters metabolism, wine fermentation, *MGL2*, *YJU3*, histone acetylation

1. Introduction

Saccharomyces cerevisiae is the main yeast species involved in the alcoholic fermentation of many beverages and foods, including bread, beer, wine, sake [1]. The secondary metabolism of fermenting yeast is the source of a broad range of volatile compounds [2] that contribute to the complex flavor of fermented beverages [3–6]. Volatile esters represent a noteworthy chemical family that was widely investigated in different beverages, since they confer a wide palette of fruity notes. The yeast enzymatic activities and the biochemical pathways involved in ester synthesis have been well described, for a review see [7,8]. Higher alcohols Acetates (HAA) result from the enzymatic condensation of acetyl-CoA and higher alcohols derived from the Ehrlich pathway [9]. This reaction is cat-

 doi:10.20944/preprints202103.0098.v1

alyzed by Alcohol Acetyl Transferases (AAT = EC 2.3.1.84) [10,11] encoded by the genes *ATF1* and *ATF2* [12]. According to several authors, the protein *Atf1p* is the most important for the production of acetate esters [12–14]. More recently, a mitochondrial Ethanol acetyltransferase Eat1p belonging to the AAT family has been characterized for its role in ethyl acetate production [15]. Fatty Acids Ethyl Esters (FAEE) result from the condensation of an Acyl-CoA component with ethanol [11,16]. This ester family is synthetized by three enzymes showing a moderate sequence divergence (*Eht1p*, *Eeb1p*, and *Mgl2p*). *Eht1p*, *Eeb1p* are Acyl-CoA:Ethanol-O-Acyl Transferase (AEATase = EC 2.3.1.75) and contribute to FAEE synthesis in a synthetic medium. The enzymatic activity of *Eht1p* has been also validated in vitro by GC-MS analyses [17]. Although sharing a high sequence homology, the third protein (*Mgl2p*) has a slighter impact on ethyl ester biosynthesis [16].

Beside these two families, Substituted Ethyl Esters have been also identified in fermented beverages. This third group is defined by the presence of substituted chains that could be alkylated and/or hydroxylated. Alkylated Ethyl Esters (AEE) (ethyl 2-methylpropanoate, ethyl 2-methylbutanoate, ethyl 3-methylbutanoate) result from the esterification of ethanol and alkyl acid derived from Ehrlich pathway [18,19]. Hydroxylated Ethyl Esters (HEE), like ethyl 2-hydroxy-4-methylpentanoate and ethyl 3-hydroxybutanoate have been also described [18,20]. Compared to their linear counterparts, substituted esters are produced in smallest quantity by *Saccharomyces cerevisiae*. However their aromatic concentration steadily increases during wine aging due to the chemical esterification by ethanol of their corresponding acids which are also produced by yeast metabolism [18,20,21]. These molecules have an important sensorial impact in red wines by enhancing fruity notes thanks to perceptive interactions phenomena [20,22,23].

In this study, the biosynthesis of substituted esters and their corresponding acids was investigated by a functional genetics approach narrowing the following genes: *ATF1*, *ATF2*, *EEB1*, *EHT1*, *MGL2* and *YJU3*. The physiological impact of several combinations of gene deletion was evaluated by implementing analytical chemistry and sensorial analyses in different red grapes grape juices. In addition, our findings highlighted genetic interactions impairing the construction of a strain deleted for all these genes. In order to understand this surprising result, a comparative transcriptomic analysis was carried out by RNA-seq approach revealing unsuspected consequences of the multiple depletion of esterase activities.

2. Results

2.1. Validation of the role of AATase and AEATase in a red wine fermentation.

All volatile compounds assayed, their chemical family and their relative abbreviations are listed in Table 1 and were measured according to methods previously developed in the laboratory [20,21,23].

 doi:10.20944/preprints202103.0098.v1

Table 1. Chemical compounds assayed by family.

Esters			Metabolic precursors		
compounds	**family**	**Abbreviation**	**compounds**	**family**	**abbreviation**
ethyl propanoate	Fatty Acid Ethyl Esters (FAEE)	C3C2	propanoic acid	Volatile Acids (VAc)	C3
ethyl butanoate		C4C2	butanoid acid		C4
ethyl hexanoate		C6C2	hexanoic acid		C6
ethyl octanoate		C8C2	octanoic acid		C8
ethyl decanoate		C10C2			
ethyl dodecanoate		C12C2			
Propyl acetate	Higher Alcohols Acetates (HAA)	C2C3	propan-1-ol	Higher alcohols (HA)	C3OH
2-methylpropyl acetate		C2iC4	2-methylpropan-1-ol		iC4OH
3-methylbutyl acetate (isoamyl acetate)		C2iC5	3-methylbutanol (isoamyl alcohol)		iC5OH
hexyl acetate		C2C6			
octyl acetate		C2C8			
2-phenylethyl acetate		C2PhC2			
ethyl 2-methylpropanoate	Alkylated Ethyl Esters (AEE)	2mC3C2	2-methylpropanoic acid	Alkylated Acids (AAc)	2mC3
ethyl 2-methylbutanoate		2mC4C2	2-methylbutanoic acid		2mC4
ethyl 3-methylbutanoate		3mC4C2	3-methylbutanoic acid		3mC4
ethyl phenylacetate		PhC2C2			
ethyl 2-hydroxy-4-methyl-pentanoate	Hydroxylated Ethyls Esters (HEE)	2h4mC5C2	ethyl 2-hydroxy-4-methyl-pentanoic acid	Hydroxylated Acids (HAc)	2h4mC5
ethyl 3-hydroxy-butanoate		3hC4C2	ethyl 3-hydroxy-butanoic acid		3hC4

The impact of Alcohol Acetyl Transferases (Atf1p, Atf2p) and Acyl-CoA:Ethanol-O-Acyl Transferase (Ehb1p, Eeb1p) in an enological context was re-assess by testing effect of the deletion of *ATF1*, *ATF2*, *EEB1* and *EHT1* in a Cabernet Sauvignon grape must. The effect of double deletions was also estimated by getting the strains Fx10-ΔA12 (*Δatf1*, *Δatf2*) and Fx10-ΔE12 (*Δeeb1*, *Δeht1*) (Table 2). At the end of the alcoholic fermentation, 18 volatile compounds were quantified by GC-MC and the results are detailed in Table S1. This set of volatile compounds encompasses 4 Acetate of Higher Alcohols (HAA), 6 Fatty Acid Ethyl Esters (FAEE), 4 AEE (Alkylated Ethyl Esters) and 4 Higher Alcohols (HA). Gene deletion did not impact the fermentation kinetics of the strain Fx10 and all the resulting wines reach similar values of residual sugar and acetic acid production (Table S1). In order to allow the easiest comparison of gene deletion, data were normalized by the average value of the control strain (Fx10). Each ester family showed a similar variation pattern according to the gene deleted as illustrated by the Figure 1a. quantitative variations are highlighted for one representative compound of each group (Figure 1b-e). HAA synthesis was drastically reduced (80 to 95%) in the Fx10-ΔA12 strain. As previously reported, the most impacting enzyme is *Atf1p* since the inactivation of *Atf2p* did not significantly impact HAA production like isoamyl acetate (C2iC5) (Figure 1b) [15]. Similarly, the esterification of C6-C12 fatty acid in FAEE is strongly reduced in the strain Fx10-ΔE12 deleted for the *EEB1* and *EHT1* genes. The main contributing enzyme is *Eeb1p* that accounts for the most part FAEE biosynthesis as illustrated for C6C2 (Figure 1c). In contrast, AEATase activity has a minor contribution in the esterification of short fatty acid (C3 and C4) since C3C2 concentration was not affected and C4C2 production was only 35% reduced in the Fx10-ΔE12 strain.

Preprints (www.preprints.org) | NOT PEER-REVIEWED | Posted: 2 March 2021 doi:10.20944/preprints202103.0098.v1

Table 2. Yeast strains used.

Strain	Background	Genotype	Description	Origin
Y31674	BY4743	*BY4743;Mata/α;his3Δ1/his3Δ1;leu2Δ0/leu2Δ0;lys2Δ0/LYS2;MET15/met15 Δ0,ura3Δ0/ura3Δ0;YOR377::kanMx4/YOR377::kanMx4*	*ATF1* deletion	Euroscarf
Y34807	BY4743	*BY4743;Mata/α;his3Δ1/his3Δ1;leu2Δ0/leu2Δ0;lys2Δ0/LYS2;MET15/met15 Δ0,ura3Δ0/ura3Δ0;YGR177::kanMx4/YGR177::kanMx4*	*ATF2* deletion	Euroscarf
Y33317	BY4743	*BY4743;Mata/α;his3Δ1/his3Δ1;leu2Δ0/leu2Δ0;lys2Δ0/LYS2;MET15/met15 Δ0,ura3Δ0/ura3Δ0;YRR177::kanMx4/YRR177::kanMx4*	*EEB1* deletion	Euroscarf
Y32157	BY4743	*BY4743;Mata/α;his3Δ1/his3Δ1;leu2Δ0/leu2Δ0;lys2Δ0/LYS2;MET15/met15 Δ0,ura3Δ0/ura3Δ0;YPL095::kanMx4/YPL095::kanMx4*	*EHT1* deletion	Euroscarf
Y30796	BY4743	*BY4743;Mata/α;his3Δ1/his3Δ1;leu2Δ0/leu2Δ0;lys2Δ0/LYS2;MET15/met15 Δ0,ura3Δ0/ura3Δ0;YMR210w::kanMx4/YMR210w::kanMx4*	*MGL2* deletion	Euroscarf
Y34943	BY4743	*BY4743;Mata/α;his3Δ1/his3Δ1;leu2Δ0/leu2Δ0;lys2Δ0/LYS2;MET15/met15 Δ0,ura3Δ0/ura3Δ0;YKL094w::kanMx4/YKL094w::kanMx4*	*YJU3* deletion	Euroscarf
Fx10 HO/ho::HYG	Fx10	*Fx10; Mata/α, HO/ho::HYG*	Diploid homozygous	ISVV collection
Fx10-ΔA1	Fx10	*Fx10; Mata/α; HO/ho::HYG; YOR377::kanMx4/YOR377::kanMx4*	*ATF1* deletion	this study
Fx10-ΔA2	Fx10	*Fx10; Mata/α, HO/ho::HYG; YGR177::kanMx4/YGR177::kanMx4*	*ATF2* deletion	this study
Fx10-ΔE1	Fx10	*Fx10; Mata/α, HO/ho::HYG; YRR177::kanMx4/YRR177::kanMx4*	*EEB1* deletion	this study
Fx10-ΔE2	Fx10	*Fx10; Mata/α, HO/ho::HYG; YPL095::kanMx4/YPL095::kanMx4*	*EHT1* deletion	this study
Fx10-ΔA12	Fx10	*Fx10; Mata/α, HO/ho::HYG; YOR377::kanMx4/YOR377::kanMx4; YGR177::kanMx4/YGR177::kanMx4*	*ATF1*, *ATF2* deletion	this study
Fx10-ΔE12	Fx10	*Fx10; Mata/α, HO/ho::HYG; YRR177::kanMx4/YRR177::kanMx4; YPL095::kanMx4/YPL095::kanMx4*	*EEB1*, *EHT1* deletion	this study
Fx10-ΔAE	Fx10	*Fx10; Mata/α, HO/ho::HYG; YOR377::kanMx4/YOR377::kanMx4; YGR177::kanMx4/YGR177::kanMx4; YRR177::kanMx4/YRR177::kanMx4; YPL095::kanMx4/YPL095::kanMx4*	*ATF1*, *ATF2*, *EEB1*, *EHT1* deletion	this study
Fx10-ΔM	Fx10	*Fx10; Mata/α, HO/ho::HYG, YMR210w::kanMx4/YMR210w::kanMx4*	*MGL2* deletion	this study
Fx10-ΔY	Fx10	*Fx10; Mata/α, HO/ho::HYG; ;YKL094w::kanMx4/YKL094w::kanMx4*	*YJU3* deletion	this study
Fx10-ΔME	Fx10	*Fx10; Mata/α, HO/ho::HYG, YMR210w::kanMx4/YMR210w::kanMx4, YRR177::kanMx4/YRR177::kanMx4; YPL095::kanMx4/YPL095::kanMx4*	*MGL2*, *EEB1*, *EHT1* deletion	this study
Fx10-ΔMY	Fx10	*Fx10; Mata/α, HO/ho::HYG, YMR210w::kanMx4/YMR210w::kanMx4, ;YKL094w::kanMx4/YKL094w::kanMx4*	*MGL2*, *YJU3* deletion	this study
Fx10-ΔAEM	Fx10	*Fx10; Mata/a, HO/ho::HYG; YOR377 /YOR377::kanMx4; YGR177 /YGR177::kanMx4; YRR177 /YRR177::kanMx4; YPL095 /YPL095::kanMx4; YMR210w /YMR210w::kanMx4*	Heterozygous hybrid for *ATF1*, *ATF2*, *EEB1*, *EHT1*, *MGL2* deletion	this study
H1xH5	Fx10	*Fx10; Mata/a, HO/ho::HYG; YOR377 /YOR377::kanMx4; YGR177 ::kanMx4/YGR177::kanMx4; YRR177::kanMx4/YRR177::kanMx4; YPL095 /YPL095::kanMx4; YMR210w /YMR210w::kanMx4*		this study
H1xH6	Fx10	*Fx10; Mata/a, HO/ho::HYG; YOR377 /YOR377::kanMx4; YGR177/YGR177::kanMx4; YRR177::kanMx4/YRR177::kanMx4; YPL095::kanMx4/YPL095::kanMx4; YMR210w /YMR210w::kanMx4*		this study
Y31674	BY4743	*BY4743;Mata/α;his3Δ1/his3Δ1;leu2Δ0/leu2Δ0;lys2Δ0/LYS2;MET15/met15 Δ0,ura3Δ0/ura3Δ0;YOR377::kanMx4/YOR377::kanMx4*	*ATF1* deletion	Euroscarf
Y34807	BY4743	*BY4743;Mata/α;his3Δ1/his3Δ1;leu2Δ0/leu2Δ0;lys2Δ0/LYS2;MET15/met15 Δ0,ura3Δ0/ura3Δ0;YGR177::kanMx4/YGR177::kanMx4*	*ATF2* deletion	Euroscarf

The production of Alkylated Ethyl Esters (AEE) was differently impacted by gene deletions. Strains with a reduced AATase activity (Atf1p, Atf2p) produce less AEE compounds with a drop of nearly 40% for 3mC4C2 and 2mC4C2 (Figure 1d and 1e, respectively). AEATase contribution (Eeb1p, Eht1p) is milder and more contrasted. While the inactivation of Eht1p reduced the production 3mC4C2 (Figure 1e), the inactivation of Eeb1p enhanced the production of 2mC4C2 and PhC2C2 (Figure 1d and 1a) suggesting a divergent contribution in the esterification of alkyl substituted acids.

 doi:10.20944/preprints202103.0098.v1

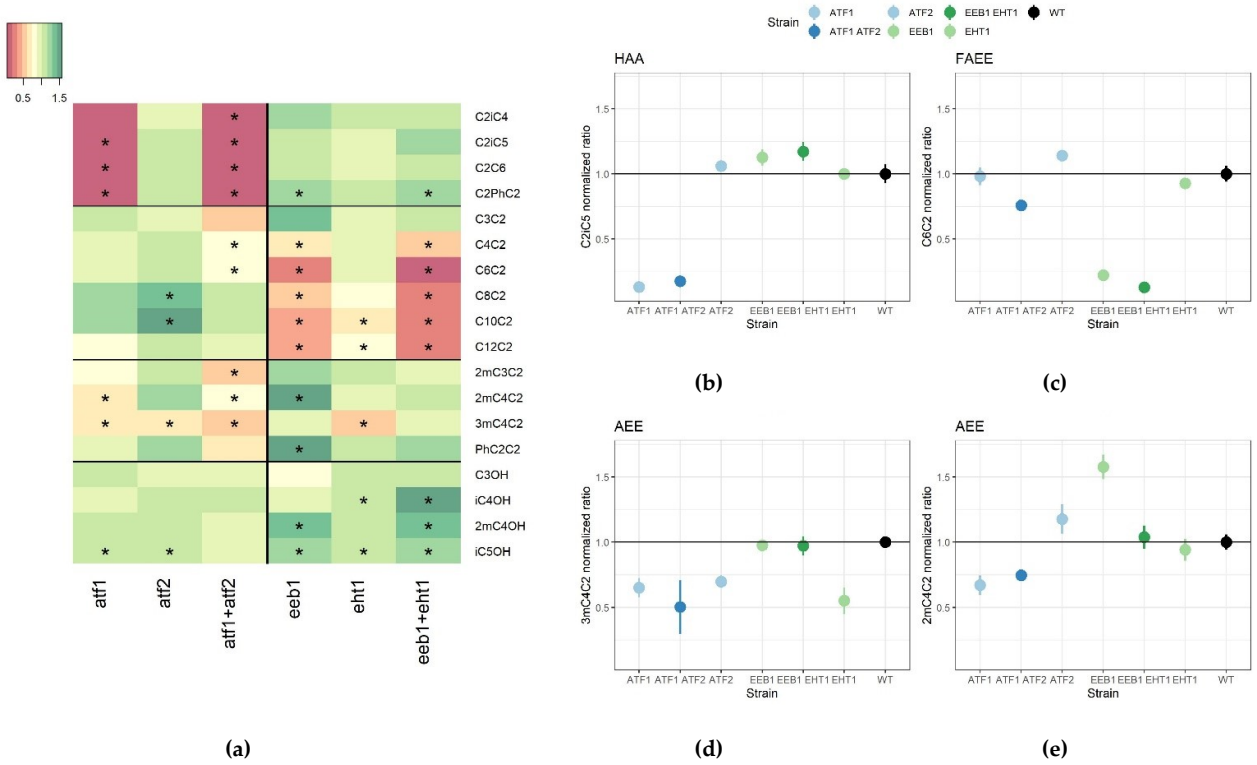

Figure 1. Depletion effect of acetyl-transferase (Atf1p/Atf2p) and acyl-CoA:Ethanol-O-Acyl transferase (Eeb1p/Eht1p) activities on linear esters. **(a)** Modalities significantly different form the *wt* were shown for all the volatile compounds measured. The symbols * indicated which modality is significantly different form the *wt* according to Kruskal-Wallis test followed by post-hoc Fisher's LSD analysis (α=0.01). **(b) - (e)** Gene deletion effects for representative compounds of each ester class family, C2iC5 (isoamyl acetate), C6C2 (ethyl hexanoate), 3mC4C2 (ethyl 3methyl butanoate) and 2mC4C2 (ethyl 2methyl butanoate), respectively. Raw values of each deletion strain were normalized by the average value of the control strain Fx10. Each point and bar represent the mean and the standard error computed from 3 to 6 independent biological repetitions.

2.2 Functional characterization of a nearly-esterase free strain

We then constructed a four deleted strain (*Δatf1*, *Δatf2*, *Δeeb1*, *Δeht1*) by crossing haploid segregants of Fx10-ΔE12 and Fx10-ΔA12 (Table 2). The resulting strain Fx10-ΔAE is isogenic to Fx10 but lacks AATase and AEATase activities. Both strains were fermented in two macerated red juices (Merlot and Tempranillo) containing a 8:2 mix of grape juice and skins. This more complex matrix better mimics the conditions of winemaking. At the end of the fermentation, 31 compounds were quantified by GC-MS and GC-FID (Table S2) including 18 esters 6 HAA, 6 FAEE, 4 AEE and 2 HEE (Hydroxylated Ethyl Esters) and 13 of their corresponding alcohols or acids: 4 Higher Alcohols (HA), 4 VAc (Volatile Acids), 3 AAc (Alkylated Acids) and 2 HAc (Hydroxylated Acids). All these molecules are produced by yeast metabolism since they were not detected in grape must (data not shown). The impact of the *strain* and *must* factors and their possible interaction was evaluated by a two-way analysis of variance (ANOVA α=0.001) (Table S3). Most part of the phenotypic variability observed was due to the strain effect since the grape must origin significant impact only two compounds (C2iC5 and 2h4mC5). This analysis confirmed that linear esters biosynthesis (except ethyl propanoate) is strongly reduced in the Fx10-ΔAE strain (Figure 2a) in agreement with results presented Figure 1. Interestingly, the combined depletion of Atf1p, Atf2p, Eeb1p, and Eht1p slightly enhanced the production of AEE (Figure 2a). In this trial Hydroxylated Ethyl Esters (HEE) were also assayed using the procedure described by Lytra et al., (2017). The strain Fx10-ΔAE showed a drastic reduction (-90%) of ethyl 3-hydroxy butanoate (3hC4C2) whatever in both grape

Preprints (www.preprints.org) | NOT PEER-REVIEWED | Posted: 2 March 2021 doi:10.20944/preprints202103.0098.v1

juices while its production of ethyl-leucate (2h4mC5C2) is not significantly impacted (Figure 2a).

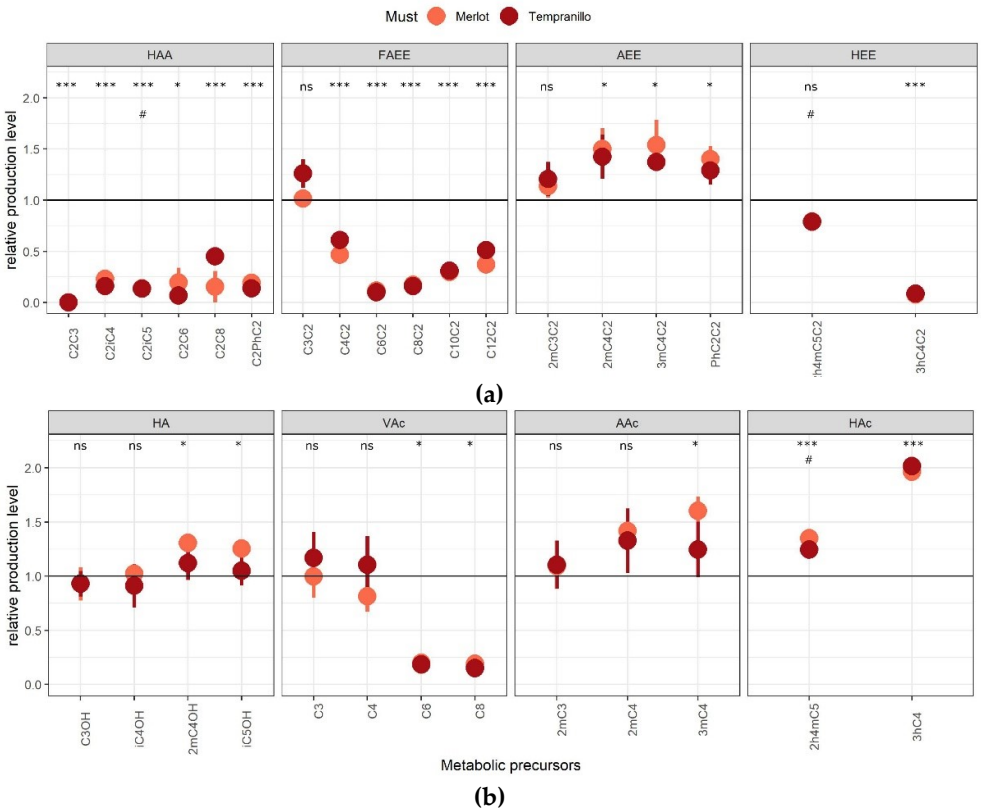

Figure 2 Relative production of esters and their metabolic precursors in one nearly esterase free strain. Raw values of the strain Fx10-ΔAE were normalized by the average value of the control strain Fx10. **(a)** the panel shows the relative production of each compounds of the four ester families in both grape musts (Merlot and Tempranillo). **(b)** the panel shows the relative production of each metabolic precursor compounds of each families in both grape musts (Merlot and Tempranillo). Each point and bar represent the mean and the standard error computed from 3 independent biological repetitions for each grape must. The symbols * and *** indicated which compounds has a significantly different production level respect to the *wt* (post hoc HSD test based on the ANOVA, α=0.05 and 0.001, respectively). The symbol # indicated which compounds has a significantly different production level according to the grape must origin (post hoc HSD test based on the ANOVA α=0.05).

The final concentrations of many esters metabolic precursors were differently impacted (Figure 2b). The production of higher alcohols (HA), linear (VAc) and substituted acids (AAc and HAc) were moderately modified, suggesting that gene deletion affects the esterification level of these molecules but not their biosynthesis. This could be explained by the fact that most volatile acids and higher alcohols are quantitatively much more abundant that their relative esters. In addition, most of them are derived from the same alpha keto acid and they concentration are likely buffered by oxidoreductive reactions. In contrast, biosynthesis of hexanoic and octanoic acids is strongly reduced (-90%) supporting the idea that the drop of C6C2 and C8C2 observed is coupled with their precursor synthesis. Finally, the production of hydroxylated acids is enhanced especially for 3-hydroxy butanoic acid that is two-folds increased in wines fermented by the Fx10-ΔAE strain (Figure 2b).

The biosynthesis pathways of hydroxylated acids and their relative esters have not yet been described before. Since they play a critical role in the evolution of fruity notes of red wines, we would determine which esterase activity is involved in their variation. According to Saerens et al. [16], a third protein (Mgl2p) may also have a

 doi:10.20944/preprints202103.0098.v1

acyl-CoA:Ethanol-O-Acyl transferase activity in *S. cerevisiae*. By deleting the *MGL2* gene in Fx10 strain and crossing it back with the Fx10-ΔE12 we obtained the triple deleted strain Fx10-ΔME (Δ*mgl2*, Δ*eeb1*, Δ*eht1*) supposed to lack any AEATase activity (Table 2). The production level of HEE was compared to the strain Fx10-ΔAE and the *wt* strain Fx10 (Figure S1). A drastic drop of 3hC4C2 was observed in both mutants demonstrating that this ester is mostly produced by AEATase. In contrast the production of ethyl-leucate (2h4mC5C2) was only slightly reduced (-15%) respect to the wild type suggesting that other enzymatic activities are involved in the biosynthesis of this ester which is both hydroxylated but also alkylated.

2.3 Sensory profiling of a wine with reduced a reduced ester content.

Merlot and Tempranillo wines produced in this experiment provide the opportunity to analyze for the first time the organoleptic impact of ester depletion in controlled conditions. Different descriptors related to the red wine fruity perception were interrogated by sensorial analysis (see methods). The panelist found a significant intensity variation for Overall Aroma (OA), Fermentative Aroma (FA), Red Fruits (RF) and Fresh Fruits (FF) descriptors. In contrast Black Fruits (BF) and Jammy Fruits (JF) notes were not significantly impacted (Wilcoxon test, α=0.05) (Figure 3). This result demonstrates that the cumulative depletion of *Atf1p*, *Atf2p*, *Eeb1p* and *Eht1p* drastically decreases fruity aromatic notes of red wine in connection with the concentration drop of linear and some substituted esters (Figure 2a). Since the production of other molecules (not assayed) might also have an effect on fruity aroma, we completed this sensorial analysis by an aromatic reconstitution. Wines fermented with Fx10-ΔAE and Fx10 strains were supplemented in various esters up to reach the same level for each ester in both supplemented wines (Table S4). A second panelist confirmed by triangular tests that wines supplemented did not shown significative differences with the control. This result confirms that the esters production discrepancy is the unique cause of the sensorial differences observed between tasted wines.

Preprints (www.preprints.org) | NOT PEER-REVIEWED | Posted: 2 March 2021 doi:10.20944/preprints202103.0098.v1

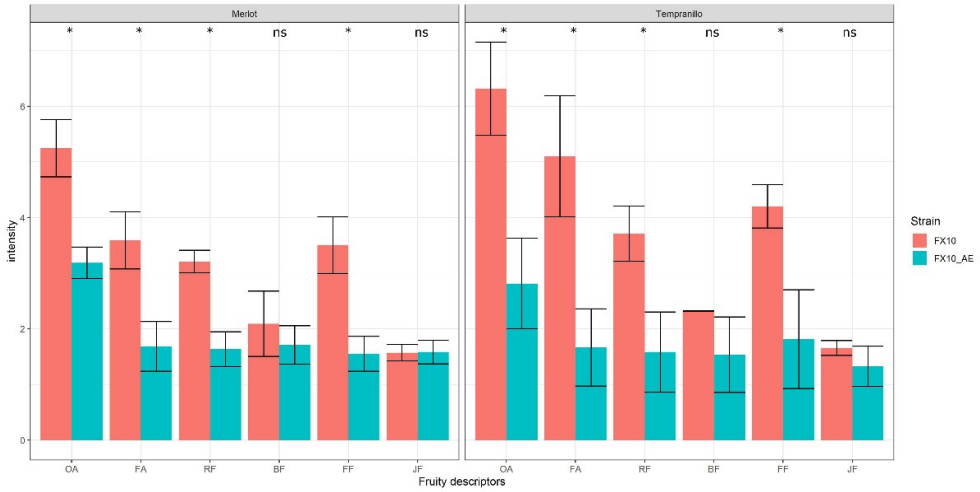

Figure 3 Sensory analysis of fruity perception of nearly ester-free wines. Wines fermented by the yeast strains Fx10 and Fx10-ΔAE were evaluated by sensorial analysis by x panelists who evaluated the intensity of different fruity descriptors: OA: Overall Aroma; FA: Fermentative Aroma; RF: Red Fruit; BF: Black Fruit; FF: Fresh Fruit; JF: Jammy Fruit. The average intensity value for each descriptor and each strain was represented for Merlot and Tempranillo wines. A Wilcoxon test was carried out for identify difference of intensity between the two strains, the symbol * indicated a significant difference (α=0.05).

2.4. Functional characterization of Mgl2p and Yju3p3, two mono-acyl glycerol lipases involved in the synthesis of substituted esters.

In the previous sections we clarified the role of AATses and AEATases on the biosynthesis of linear esters and 3hC4C2. However, AEE and ethyl leucate biosynthesis have not been yet completely elucidated. Beside *Atf1p*, *Atf2p*, *Eeb1p* and *Eht1p*, other enzymes may play a role on substituted ester biosynthesis. We hypothesized that the two proteins *Mgl2p* and *Yju3p* could modulate the concentration of fatty acids which are the precursors of ethyl esters. Indeed, these proteins have been characterized for their Mono-Acyl Glycerol Lipase (MAGLase) activity [24,25]. To test this hypothesis, the same functional genetic strategy was applied and both enzymes were inactivated in the strain Fx10-ΔM (*Δmgl2*) and Fx10-ΔY (*Δyju3*). Their combined effect was also evaluated in the double mutant Fx10-ΔYM (*Δyju3, Δmgl2*) (Table 2). Again, the fermentation kinetics of such strains was similar to the control (data not shown). The depletion effect of MAGLase activity is summarized by a heat map (Figure 4a). Mgl2p and Yju3p had a very moderate role in the biosynthesis of linear esters of fatty acids and did not influence the production level of higher alcohols and their corresponding acetate esters (Figure S2 a and b). Although significative, the inactivation of MAGLases had only a slight effect of FAEE production (-10%) (Figure S2 c and d) compared to AEATses inactivation (Figure 1 and 2). In contrast, MAGLase are significantly involved in the *de novo* synthesis of most substituted ethyl esters. Indeed, AEE production is reduced by nearly 50% compared to the control in single and double mutants (Kruskal-Wallis test α=0.01) (Figure 4b). However, the double deletion of *MGL2* and *YJU3* does not abolish AEE production suggesting that other enzymes (including *Eeb1p* and *Eth1p*) compensate their inactivation. Remarkably, *Mgl2p* and *Yju3p* did not affect the production level of a phenyl-substituted esters (PhC2C2) that seems to be produced by an alternative route (Figure 4a). The biosynthesis of hydroxylated esters showed a more contrasted genetic determinism. Ethyl-leucate (2h4mC5C2) is reduced by nearly 50% in the double mutant (Figure 4c) but as observed for alkylated esters, its production is not fully abolished. This drop positively coupled with the biosynthesis of its corresponding acid (2h4mC5) (Figure 4c). This suggests that MAGL may control the biosynthesis of the ethyl 2-hydroxy-4-methylpentanoic acid which in turn influences the production level of ethyl-leucate. In contrast, the production level of ethyl-3

 doi:10.20944/preprints202103.0098.v1

hydroxy-butanoate (3hC4C2) was not evenly impacted by MAGL inactivation. *MGL2* deletion promoted 3hC4C2 synthesis (+50%) while *YJU3* deletion had no impact with a dominant effect on *MGL2* (Figure 4c). Altogether, these findings demonstrate for the first time the impact of MAGLase activity on the biosynthesis of volatile substituted esters in the context of the alcoholic fermentation.

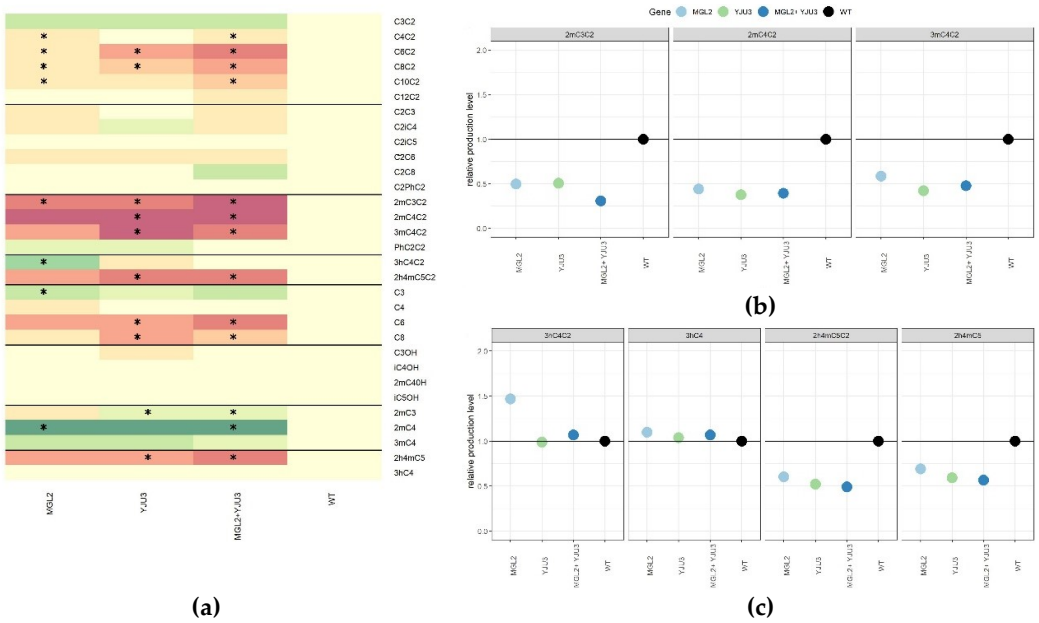

Figure 4 Depletion effect of mono-acyl glycerol lipases activities (Mgl2p/Yju3p) on substituted esters and their relative metabolic precursors. Raw values of each deletion strain (*MGL2* and/or *YJU3*) were normalized by the average value of the control strain Fx10. **(a)** modalities significantly different form the *wt* were shown for all the volatile compounds measured. **(b)** deletion effect for significantly impacted AEE. **(c)** deletion effect for HEE and their relative precursors. Each point and bar represent the mean and the standard error computed from 4 independent biological repetitions measured in two grape juices. The symbols * indicated which modality is significantly different form the *wt* according post hoc HSD test (α=0.001).

2.5. Attempts to construct a fully esterase-free yeast strain.

The possible metabolic connections between enzymatic activities (AATase, AEATase and MAGLase) prompted us to integrate in the Fx10-ΔAE strain the *MGL2::KanMx* allele that significantly impacts AEE and HEE biosynthesis. Using a breeding strategy, an F1 hybrid (Fx10-ΔAEM) was obtained by crossing appropriated haploid segregants of Fx10-ΔAE and Fx10-ΔM. Since deleted genes are located in different chromosomes, the expected frequency of a Fx10-ΔAEM progeny with the five-deleted genes would be 1/32. Surprisingly by genotyping such progeny by PCR, we failed to identify any segregant harboring all the five deleted genes in the 296 spores dissected (Figure 5a). In order to increase the chance to get such progeny, different combinations of Fx10-ΔAEM segregants were crossed each together aiming to fix some desired alleles. Surprisingly for some haplotype combinations, the isolated F2-zygotes did not develop a central bud and stopped their growth at the first division stage. This prezygotic incompatibility was visually observed in three haplotype combinations (H1xH2; H1xH3 and H3xH6) in 70 distinct zygotes (Table 3). In contrast, other crosses (H1xH5 and H1xH6) developed zygotes with a perfect fitness. The sporulation of these viable F2-hybrids (H1xH5 and H1xH6) would also allow the isolation of segregants carrying the five deleted genes with a frequency of 1/8. Among the 176 progenies dissected, we failed to obtain a strain deleted for the five genes (*Δatf1*, *Δatf2*, *Δeeb1*, *Δeht1*, *Δmgl2*). In these two F2-hybrids, seven pairs of double mutants were expected with a frequency of 50% (Figure 5b). Surprisingly the

 doi:10.20944/preprints202103.0098.v1

double mutant *Δatf1,Δmgl2* was scarcely represented (5%) compared to other combination pairs (chi square test $p=1.10^{-7}$) indicating a probable deleterious interaction. However, this interaction cannot be considered as synthetic lethality since some *Δatf1,Δmgl2* strains have been isolated in Fx10-ΔAEM progeny (haplotypes H2 and H3). Another noteworthy result is the low germination percentage of hybrids dissected (between 82 and 75 %) which is quite unusual in nearly isogenic crosses. By typing all the progenies dissected, we inferred the genotype of non-viable clones. Most of them would have the "five deleted genes" pattern sought (data not shown). These findings strongly suggest that the combined loss of *MGL2* and *ATF1* genes confers a drastic and unexplained loss of viability.

Table 3. Summary of haplotypes tested.

Pedegree	ploidy	haplotype[1]	viable	unviable	number of functional copies				
					ATF1	ATF2	EEB1	EHT1	MGL2
Fx10-Delta5-progeny	n	H1	5	0	0	0	0	0	2
	n	H2	1	0	0	2	2	2	0
	n	H3	1	0	0	2	2	0	0
	n	H4	1	0	2	0	0	0	0
	n	H5	2	0	2	2	0	0	0
	n	H6	2	0	2	0	0	2	0
F2-hybrids	2n	H1/H2	0	20	0	1	1	1	1
	2n	H1/H3	0	20	0	1	1	0	1

[1] for the viable strain, haplotypes were verified by PCR; for the unviable background they were inferred from parental genotype.

Preprints (www.preprints.org) | NOT PEER-REVIEWED | Posted: 2 March 2021 doi:10.20944/preprints202103.0098.v1

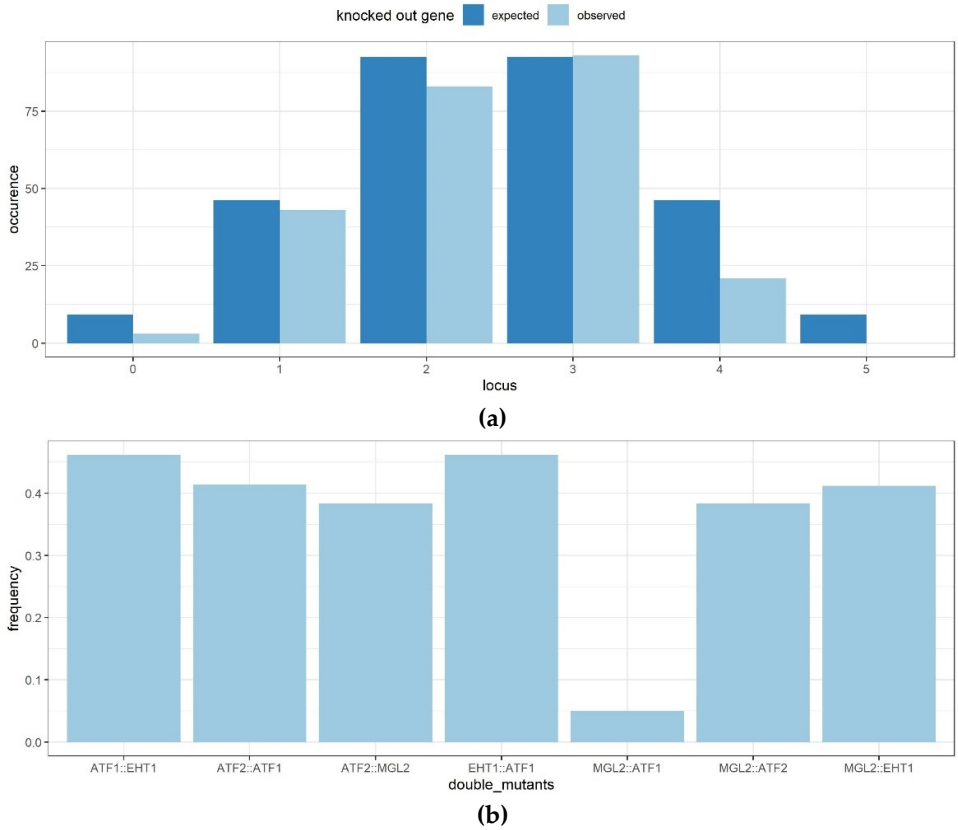

Figure 5 Genetic interactions between esterase genes impair the development of a multiple deletion strain. **(a)** Observed (light blue) and expected (dark blue) occurrences of meiotic progeny of the Fx10-ΔAEM (*ATF1*/*Δatf1*, *ATF2*/*Δatf2*, *EEB1*/*Δeeb1*, *EHT1*/*Δeht1*, *MGL2*/*Δmgl2*) harboring 0 to 5 knocked out genes. **(b)** Frequencies of meiotic segregants of the hybrids H1xH5 and H1xH6 showing a double deletion for the genes *ATF1*, *ATF1*, *EEB1*, *EHT1* and *MGL2*. *** indicated a significative difference respect to the expected ratio of 0.5(chisquare test α =0.001)

2.6. Transcriptomic analysis of the Fx10-ΔAE strain reveals the unsuspected consequences of the depletion of esterase activities.

Genetic incompatibility revealed in the previous section contrasted with the absence of macroscopic phenotypes in strains deleted for one or many esterase genes. For instance, the strain Fx10-ΔAE (*Δatf1*, *Δatf2*, *Δeeb1*, *Δeht1*) shows a very similar fermentation kinetics than Fx10 (data not shown). This surprising result prompted us to deeply investigate the physiological consequences of multiple gene deletion by a transcriptomic approach. Biomass of strains (Fx10-ΔAE and Fx10) was collected at 30% of the alcoholic fermentation (Merlot grape juice) and total RNA was extracted and the corresponding cDNAs were sequenced by Proton technology (see methods). RNA sequencing allowed the quantification of 6287 genes commonly detected. The average fold change ratio log2 (Fx10-ΔAE/Fx10) was computed and genes showing a statistical difference were defined by ANOVA or Kruskal-Wallis test (whenever ANOVA assumptions were not met). This analysis identified 1124 Differentially Expressed Genes (DEG) showing a significative difference with at least a two folds change expression. This result suggests that combined deletion of four genes trigger an important transcriptome remodeling. Surprisingly, a strong bias toward genes overexpression in the strain Fx10-ΔAE was found since 1102 and 22 genes were up and down regulated, respectively (Figure 6a and Table S5). As expected, *ATF1*, *EHT1* and *EEB1* were part of the shut-down genes since very few reads were mapped at their positions. Initially, *ATF2* did not appeared as DEG (Figure 6B). A closer scrutiny revealed that *ATF2* overlapped partially with another ORF, *YGR176W*. In

Preprints (www.preprints.org) | NOT PEER-REVIEWED | Posted: 2 March 2021 doi:10.20944/preprints202103.0098.v1

order to correctly quantify *ATF2* only, overlapping reads between *ATF2* and *YGR176W* were subtracted, revealing an actual absence of *ATF2* mRNA in the Fx10-ΔAE mutant (Figure 6b). This first analysis confirms the correct and complete deletion of the four genes in the strain Fx10-ΔAE. Interestingly, the gene *MGL2*, was identified as up-regulated in the Fx10-ΔAE mutant, suggesting the existence of mechanisms of dosage compensation between esterase genes. In addition, *YJU3* the second MAGL gene investigated in this study, was also significantly up-regulated in the mutant (p-value<0.05). Since it showed a small increase (44%, less than two-fold change) this gene was not considered as DEG in further analyses.

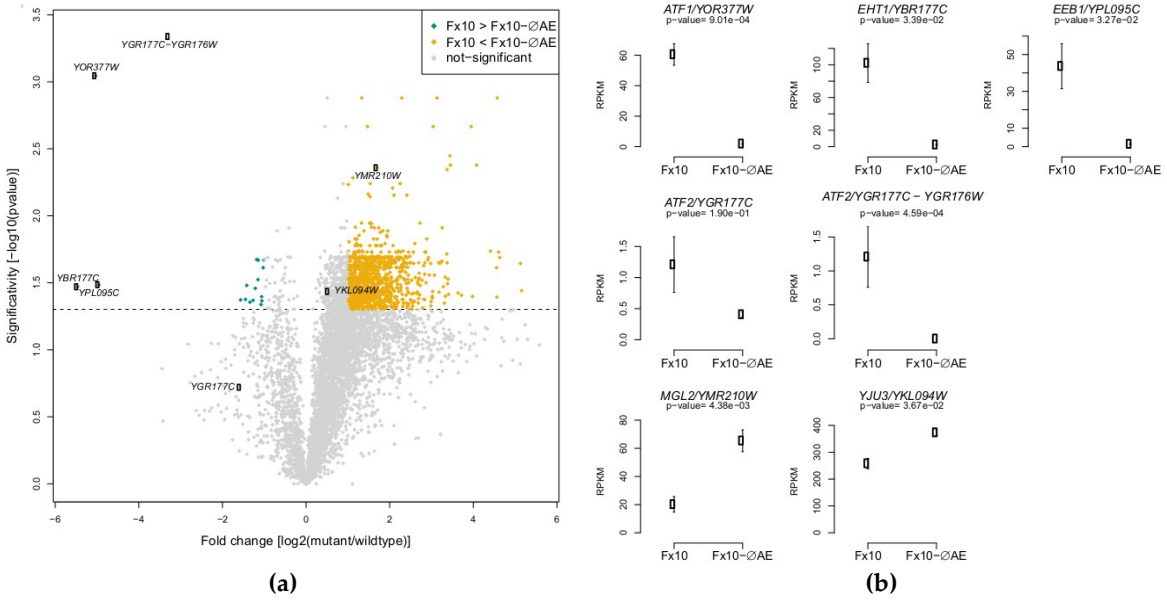

Figure 6. RNA-seq analysis of the Fx10-ΔAE mutant. **(a)** Volcano plot showing differentially expressed genes in the Fx10-ΔAE mutant compared to the Fx10 wildtype strain. 6287 genes were considered, of which 1124 were DEG. Yellow and blue-green dots show the 22 and 1102 genes down-regulated or up-regulated in the mutant, respectively. Grey dots represent the 5163 non-significant genes. **(b)** Expression patterns for genes of interest in the Fx10 wildtype and the Fx10-ΔAE mutant. RPKM stands for Reads Per Kilobase Million. Error bars represent standard errors. P-values were corrected for FDR multiple tests.

A gene ontology (GO) analysis identified 23 GO categories that were significantly enriched or depleted in differentially expressed genes (hypergeometric distribution with Holm-Bonferroni correction, α=0.05). Interestingly, most of the GO categories concern major biological processes involved in cellular housekeeping functions including mRNA and rRNA processing (GO:0006397, GO:0006364), cell division (GO:0051301), transmembrane transport (GO:0055085), and oxidoreduction process (GO:0055114). The strong enrichment in genes related to RNA metabolism is also confirmed by a significative enrichment in RNA binding function (GO: 0003723) as well by the fact that half (517) of the 1124 genes were associated with the nucleus (GO:0005634) which is three times more that the proportion expected for the whole genome (Figure S3). This first analysis reveals that the deletion of the main esterase genes triggers an unexpected modification of genome expression in the strain Fx10-ΔAE. In order to unravel this surprising expression repatterning we sought functional connections between DEGs by interrogating the Protein-Protein Interactions (PPI) database (string-db.org). A cluster analysis of the PPI score matrix allowed the identification of 13 PPI clusters sharing functional relationships (Figure 7). Each cluster encompasses more than 14 proteins and reaching an average score higher than 0.51. Most of them (clusters 1, 2,6, 7, 8, 10, 11, 12) were enriched in protein networks related nitrogen and lipid metabolism (GO:0006807, GO:1901564, GO:1901566, GO:0006629). This connection with metabolism was not directly identified

Preprints (www.preprints.org) | NOT PEER-REVIEWED | Posted: 2 March 2021 doi:10.20944/preprints202103.0098.v1

by the GO enrichment analysis, highlighting the interest of using PPI score to discover functional components in genome-wide datasets. Interestingly, the cluster 13 encompasses 14 proteins mostly involved in lipid metabolism and Acyl transferase activity (GO:0016746), including the MAGLase *Mgl2p*. This result demonstrated that the lack of AATses and AEATase activities triggers the expression of many genes involved in amino acid and lipid biosynthesis pathway.

Other PPI clusters were related to RNA regulation (clusters 1, 2 and 6, GO:0016070), mitochondrion and mitochondrial translation (clusters 5 and 10, GO:0005739, GO:0032543), cell cycle (cluster 3, GO:0007049), site of polarized growth (cluster 9, GO:0030427), congruently with previous GO analysis. A few other elements were identified by PPI analysis: response to stimulus (cluster 4, GO:0050896), cellular aromatic compound metabolic process (GO:0006725) and the involvement of phosphoprotein (clusters 3, 4 and 9, KW-0597). Finally, the cluster 12 in particularly enriched in proteins involved in covalent chromatin modification (CL:3190) encompassing proteins belonging histone acetyltransferase (CL:3659) and histone deacetylase (CL:3384) complexes (https://version-11-0b.string-db.org/cgi/network?networkId=b8KiKTUhCG3I).

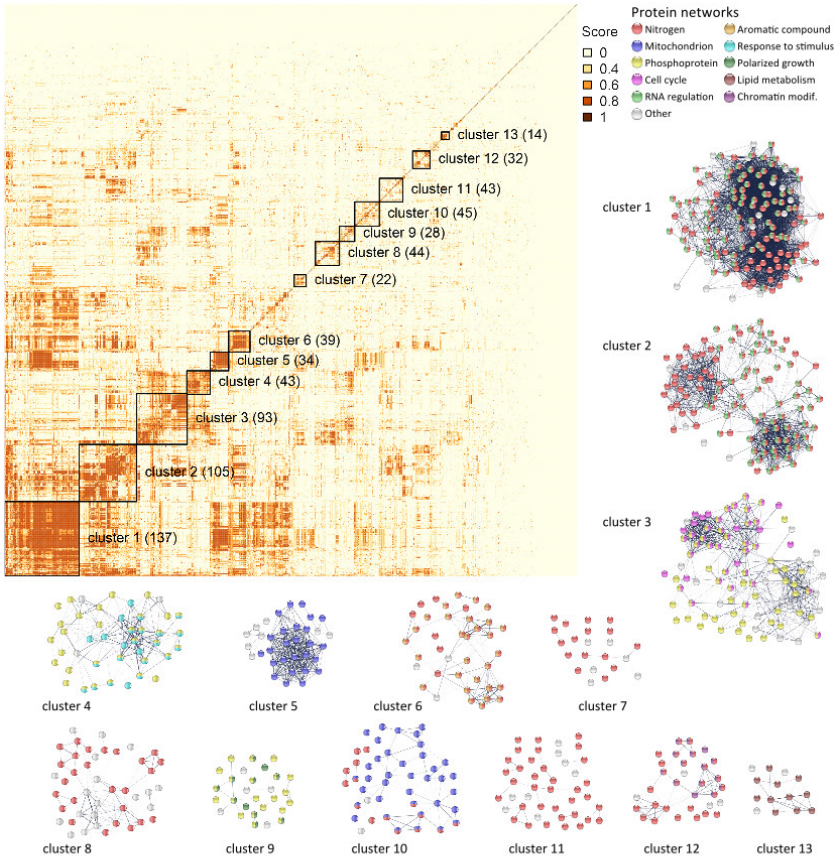

Figure 7 STRING protein-protein interactions analysis. Clustered pairwise correlation matrix (top,left) of the 1124 differentially regulated genes in the Fx10-ΔAE mutant. For each pair of genes, a protein-protein interaction (PPI) confidence score was extracted from STRINGdb (http://string-db.org/). 13 clusters were visually defined (the number of proteins per cluster is shown in brackets), and the STRING PPI network connectivity was represented. For each cluster, the main functional enrichment(s) of the networks (biological process from gene ontology, local network cluster from STRING or annotated keywords from UniProt) were represented by different colors.

Preprints (www.preprints.org) | NOT PEER-REVIEWED | Posted: 2 March 2021 doi:10.20944/preprints202103.0098.v1

The presence of proteins related to chromatin modification and the wide overexpression pattern of the strain Fx10-ΔAE lead us to check possible connection with histone modifications by interrogating a dataset of nucleosome co immuno-precipitation [26]. The average ratios of acetylation and methylation in up- and down-regulated genes were compared to those of non-significant genes (Figure 8). Most histone modifications were significantly affected in the mutant, with 7 upon 8 modifications enriched in the pool of up-regulated genes. Accordingly, down-regulated genes were depleted in histone modifications (5/8). This general trend is consistent with the fact that histone modifications like acetylation or methylation are frequently associated with increased transcriptional activities and chromatin structure. Altogether, these results underline a significant disturbance of histone modification and chromatin structure in the Fx10-ΔAE mutant, congruent with the high number of up-regulated genes in this strain.

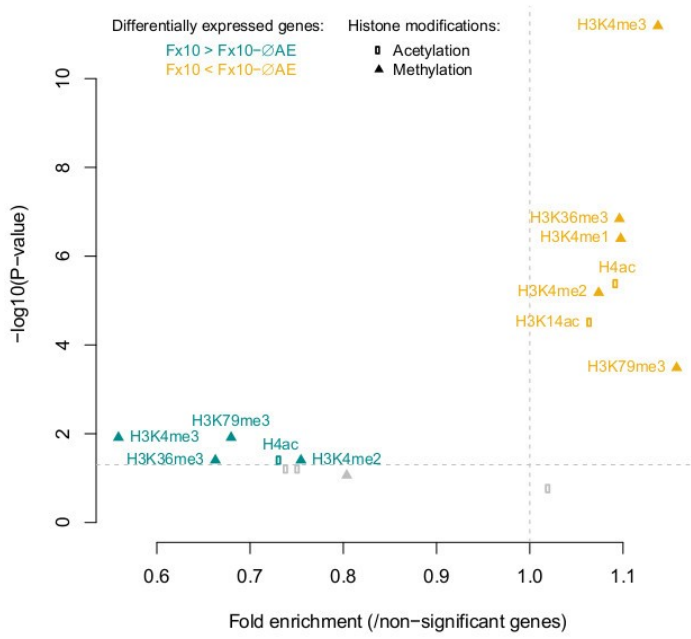

Figure 8. Enriched or depleted histone modifications in the Fx10-ΔAE mutant. Possible histone modifications (3 acetylations and 5 methylations) were searched for all genes. The average ratios of acetylations and methylations in up- and down-regulated genes were compared to those of non-significant genes (Kruskal-Wallis tests). P-values were corrected for multiple testing with Benjamin-Hochberg adjustment. Not-significantly enriched/depleted histone modifications are shown in grey, while significant ones (P-value<0.05) are colored. The histone modifications data was available from [26]

3. Discussion

3.1. General reassessment of the esterase contribution in red wine making condition.

Although esters are very impacting compounds of wine flavor, the functional characterization of genes and enzymes involved in their biosynthesis was rarely achieved in natural grape juices. Indeed, the genetic basis of ester biosynthesis has been evaluated in culture broths (YPD, YNB) [12,16,27] or in synthetic grape juice [28]. Since the nitrogen composition has strong impact on esters metabolism [29,30], the use of artificial media may create physiological biases respect to natural grape juices. This discrepancy has been recently confirmed by comparing the gene deletion of several genes in laboratory culture broth and in white grape juice [15]. By analyzing the deletion effect of six genes in an enological context, we clarified their role in the biosynthesis on linear and substituted

Preprints (www.preprints.org) | NOT PEER-REVIEWED | Posted: 2 March 2021 doi:10.20944/preprints202103.0098.v1

esters including HEE that were never considered before. In order to draw robust conclusions, gene deletion effects were evaluated in three different matrixes (Cabernet Sauvignon, Merlot and Tempranillo). The use of a fully homozygous diploid background (Fx10) allows the convenient construction of simple and multiple deleted strains by combining genetic engineering and classical breeding approaches. The Figure 9 summarizes their relative contributions in the biosynthesis of ester classes considered in this study.

Ester family	compounds	AATase	AEATase	MAGLase	AATase & AEATase
HAA	C2C3	nd	nd	=	×
	C2iC5, C2C6, C2iC4	×	=	=	×
	C2PhC2	×	↗	=	×
FAEE	C3C2	=	=	=	=
	C4C2	↗	↘↘	↘	↘
	C6C2-C12C2	=	×	↘	↘↘
AEE	2mC3C2	↘	=	↘↘	=
	2mC4C2	↘	↗	↘↘	↗
	3mC4C2	↘	↘	↘↘	↗
	PhC2C2	=	↗	=	↗
HEE	3hC4C2	=	↘↘	=	↘↘
	2h4mC5C2	=	↘	↘↘	↘

Reduction:
more than 25% ↘
more than 50% ↘↘
more than 75% ×

Increasement:
more than 25% : ↗

No effect: =

Figure 9. Relative contributions of AATses, AEATases and MAGLases to the biosynthesis of volatile esters in a wine-making context.

The inactivation of AATses (Atf1p and Atf2p) and AEATses (Eeb1p, Eht1p) confirmed their respective role in the biogenesis of HAA and FAEE compounds. Both pathways are quite independent since the depletion of one class of enzyme has a null or very moderated effect on the biosynthesis of the other group, except for the acetate of phenyl-ethanol and ethyl-butanoate that were slightly enhanced by the inactivation of AEATses and AATses, respectively. When both enzymatic activities are inactivated (strain Fx10-ΔAE), linear ester biosynthesis is drastically reduced especially for HAA. In contrast, the biosynthesis of ethyl propanoate (C3C2) was not affected at all. In a recent study, the production of this ester has been linked to a mitochondrial Ethanol acetyltransferase Eat1p. *EAT1* overexpression increase the biosynthesis of ethyl propanoate by condensing ethanol and propionyl-CoA [15]. However, according to the same authors, the deletion of this gene does not impact its biosynthesis in grape juice likely due to a low oxygenation level.

Beside the well documented biosynthesis of linear esters, this study focuses on substituted esters metabolism that contribute to the fruity notes of young red wines [20,23]. Our investigations demonstrated that yeast esterases (Atf1p, Atf2p, Eeb1p, Eht1p) are not the main contributors of AEE and HEE biosynthesis. Indeed, the esterification of alkyl substituted acids in enological conditions (2-methyl-propanoate, 2-methyl butanoate, and 3-methyl butanoate) are poorly impacted by AATases inactivation (-25%). Since AATase catalyze the condensation of Acetyl-COA and higher alcohols, their impact on substituted ethyl ester is likely indirect and should be due to metabolic connections existing between methylated alcohols and methylated acids that are derived from the respective reduction and oxidation of methyl substituted aldehydes [31]. AEATases have a more contrasted role since the production of some alkyl esters is reduced (3mC4C2) or

enhanced (PhC2C2). It is important to note that the concentrations measured for this last compounds are quite low and would not impact the sensory profile of wines. Although Eeb1p and Eht1p does not efficiently catalyze the esterification of Alkylated Acids, they are clearly involved in the biosynthesis of ethyl 3-hydroxy-butanoate (Figure 2 and Figure S1)which confers red-berry and fresh-fruit notes, even at subthreshold concentrations [32].

The reassessment of substituted ethyl esters metabolism was completed by evaluating the role of two MAGLases. The deletion of *MGL2* and *YJU3* reduced drastically the biosynthesis of methyl substituted esters such as 2mC3C2, 2mC4C2, 3mC4C2 and 2h4mC5C2. In the particular case of ethyl leucate biosynthesis, MAGLases inactivation also reduced the concentration of its direct precursor 2-hydroxy-4-methyl pentanoic acid, which is not observed for the other methylated acids. This result suggests that the direct precursor of ethyl-leucate may be derived from the degradation of lipids metabolism which is consistent with the primary function of Mono Acyl Glycerol lipases.

To date, sensorial consequences of esters depletion were never investigated in red wines. By fermenting the strain Fx10-ΔAE in two macerated grape juices we demonstrated by sensorial analyses that esters depletion has a significant effect on various aromatic descriptors by reducing the perception of red and fresh fruit notes as well as the overall aroma of wines tasted. Aromatic reconstruction carried out with synthetic molecules demonstrated that the drop fruity perception observed was due to the depletion ester itself, discarding the hypothetical impact of hidden compounds not assayed.

3.2. Genetic and transcriptomics experiments reveal unsuspected physiological consequences of esterase activity.

Unexpectedly, we failed to get a strain deleted for all the six genes investigated. As colleagues [15], the construction of a four deleted strain Fx10-ΔAE (*Δatf1*, *Δatf2*, *Δeeb1*, *Δeht1*) was readily achieved by a breeding approach. However, we repeatedly fail to isolate a strain carrying a fifth deletion (*Δmgl2*) using independent strategies (cross or segregation). Strikingly, for several haplotype combinations all the zygotes isolated did not develop a central bud or stop their growth at the first division step suggesting a possible deficiency in cell polarization or in bud formation. This result led us to deeply investigated the physiological changes provoked by the deletion of the four main esterases. At the macroscopic level, no significative change respect to the control were observed: both strains have a similar fitness in broth media and grape juice. In contrast, strong variations were measured at the transcriptomic levels since more than 1100 DEG were clearly identified. The significative overexpression of *MGL2*, and in a less extent of *YJU3*, suggests the existence of genetic compensation mechanisms in the context of esterases depletion. As a consequence, the deletion of *MGL2* could impairs such compensations having a synthetic lethal effect in the Fx10-ΔAE background. This deleterious effect is observed when all the five genes are deleted supporting the idea Mgl2p, Eeb1p, Eht1p, Atf2p and Atf1p share complementary functions. Although we did not identify a precise genetic interaction, the strong reduction of germination rate for progeny carrying the *Δmgl2* and *Δatf1* alleles support the idea that these two genes could ensure a crucial role in yeast viability by unknown mechanism.

In phase with this genetic incompatibility, a preliminary transcriptomic analysis confirms that the drastic reduction of ester production is not neutral in term of molecular physiology. Indeed, the strain Fx10-AE showed a drastic expression repatterning with a strong bias toward gene overexpression (1002 vs 22 genes). GO enrichment and PPI STRING analyses depicted a large set of activated pathways. On the first hand, many genes involved in nitrogen and lipid metabolism were identified. In particular, esterase inactivation enhanced the expression of genes related to basic and aliphatic amino acid biosynthesis such as lysine (*LYS14*, *LYS20*, *LYS2*, *LYS9*), arginine (*ARG4* and *ARG8*), methionine (*MET31*), leucine (*LEU5*) and threonine (*THR4*) (File S8). The transport of these amino acids is also enhanced with the overexpression of basic and substituted

amino acid transporters (*VBA3*, *VBA5*, *BAP3*). In addition, PPI analysis identified a small cluster of 14 genes related to lipid metabolism including *MGL2* and *YJU3*. Most of them are involved in triglyceride homeostasis and lipid droplet formation (*CST6*, *LOA1*, TGL2, *TGL3*, *TGL5*) and were annotated for their Acyl-transferase activity that could compensate the deletion of *EEB1* and *EHT1*. Beside these broad metabolic adjustments, many genes overexpressed are related to central cellular functions such as cell cycle and polarization as well as RNA binding. The detection of a small cluster of 32 proteins (cluster 12) involved in chromatin modification retained our attention. This group encompassed key components (*HAD2*, *CTI6*, *AHC2*, *EAF7*) of two protein complexes involved in histone acetylation and deacetylation, HAD1 and ADA, respectively [33]. Since all genes were overexpressed in the mutant, we hypothesized that Fx10 ΔAE had an abnormal chromatin acetylation explaining the expression repatterning observed. This hypothesis is corroborated by the fact that the DEG set is more subject to histone acetylation than the rest of the genome. Since histone methylation and acetylation are partially correlated, the DEG set is also more subject to histone methylation. A possible link between histone modification and ester formation is the Acetyl-CoA molecule itself that constitute a common substrate for acetyl histone transferases and AATses. In yeast, the level of acetyl-CoA is tightly regulated by acetyl-CoA synthetase (Acs1p, Acs2p) and acetyl-CoA hydrolase (Ach1p). We hypothesized that AATses could also reduce acetyl-CoA pool by producing acetate esters of higher alcohols. Therefore, in the Fx10-ΔAE strain, ATAses inactivation would increase the nucleocytosolic pool of acetyl-CoA triggering histone acetylation which consistent with an overall elevation of gene expression.

4. Materials and Methods

4.1. Culture conditions and classical genetics manipulations

All the strains of this study belong to the *Saccharomyces cerevisiae* species and were propagated at 28°C on YPD medium (1% yeast extract, 2% peptone, dextrose 2%) complemented with 2% agar to prepare solid medium. *KanMx* and *HygMx* markers were selected by using G418 (100µg/mL) and hygromycin B (300 µg/ml), respectively. Sporulation was induced in ACK medium (potassium acetate 1%, agar 2%) at 24°C for three days and free spores were obtained by a cytohelicase treatment (2 mg/L, 90 min at 30°C). Cell mating was performed by incubating 10^5/ml of spores and/or haploid cells in YPD for 6 h at 30°C. Newly formed zygotes were then isolated from the mix by micromanipulation using a Singer apparatus MS200. The Mendelian segregation of deleted genes was controlled by analyzing at least four complete tetrads isolated by micromanipulation.

4.2. Construction of esterase-free yeast strains

A collection of nine *knocked-out* strains isogenic to the Fx10 background was obtained (Table 2). This strain is a commercial starter Zymaflore Fx10 (Laffort, France), that is widely used for red juice fermentation. This diploid, homothallic, and fully homozygous strain has been previously used by our laboratory [34]. The deletion of the six genes of this study (*ATF1*, *ATF2*, *EEB1*, *EHT1*, *MGL2*, *YJU3*) has been achieved by using PCR-deletion cassettes obtained by amplifying the genomic DNA of the Euroscarf collection strains Y31674, Y34807, Y33317, Y32157, Y30796 and Y34943, respectively. The strain Fx10 was transformed using an optimized lithium acetate protocol [35]. All constructions were verified by an appropriate insertion PCR. Briefly, the verification consisted in positively amplifying by PCR a fragment containing ~600 pb of the 5'-flanking region and the 5' part of the *KanMx4* cassette. All the primers used for this test are listed in Table S6. Multiple deletion strains were obtained by meiotic segregation and iterative cross with appropriate deletion mutants. Meiotic segregants were selected based on G418 resistance and verified for both marker insertion and gene deletion using appropriate PCRs. To simplify the cross procedure, a haploid isogenic clone of Fx10 (YMP34) was

used. This strain has been deleted for the *HO* gene by the *ho::HygKx4* cassette allowing to select readily F1 hybrids with G418 resistant strains [34].

4.3. Fermentation conditions

Two distinct fermentation batches were carried out. Simple and double deletion mutants of genes involved in linear ester biosynthesis were tested in a thermo-treated grape juice of Cabernet sauvignon (CS) harvested in 2013 in the Bordeaux area and conserved at -20°C. Assimilable nitrogen concentration of this grapes juice was 200 mg N/L with mixed sources of amino acid and ammonium nitrogen (60/40 ratio). Fermentation took place in cylindric glass-vessels of 300 ml with permanent stirring (200 rpm).

A second batch of fermentation was carried out in larger volumes in order to test the organoleptic impact of gene deletion. Two different grape varieties harvested in 2015 were used: a Merlot (Bordeaux area, France) and a Tempranillo (Rioja area, Spain). In order to mimic red-grape vinification, a specific protocol was developed. Full grapes were destemmed, crushed, pressed and both the juice and the skins were conserved separately. Before freezing, potassium metabisulfite was added to the must for reaching 50 mg/L of total SO_2. For both grape varieties, sugar concentration was set up to 230 g/L of reducing sugar by adding an equimolar amount of D-glucose and D-fructose. Assimilable nitrogen concentration was also adjusted at 210 mgN/L respecting the balance between amino acids and ammonium nitrogen source kept to 66:34 by using a solution of 18 α-amino acids and $(NH_4)_2SO_4$ as previously described [36]. These fermentations took place in 2.5 L cylindric glass flasks filled with 1.6 L of juice and with 400 mL of grape skin in order to keep a juice/solid ratio of 80:20, usual in oenology, each flask was mixed twice a day.

In all fermentation batches, grape juice was inoculated with 1.10^6 viable cell/mL obtained from 24h-precultures carried out in half-diluted grape must sterilized by membrane filtration (cellulose acetate 0.45 µm Sartorius Stedim Biotech, Aubagne, France). Yeast viability and concentration were estimated by flux cytometry "Cell Lab Quanta SC" (Beckman Coulter, USA, California) according to the procedure previously described [37]. Fermentation kinetics were monitored by CO_2 release [38]. At the end of the alcoholic fermentation, wines were collected in glass bottles and stored at 10°C for 1 week after the addition of SO_2 (50mg/L).

4.4. Total RNA isolation and mRNA sequencing

Fermenting yeast were aseptically sampled at 30% of the alcoholic fermentation to achieved RNA seq analysis. Cells were pelleted by centrifugation, washed 4 time and frozen at -80°C. Since the grape must was rich in polyphenols and anthocyanins the mRNAs were extracted according to the Reid's procedure (2006) adapted for yeast. The extraction buffer contained 300 mM Tris HCl (pH 8.0), 25 mM EDTA, 2 M NaCl, 2% CTAB, 2% PVPP, 0.05% spermidine trihydrochloride, and just prior to use, 2% β-mercapto-ethanol. Yeasts were ground to a fine powder in liquid nitrogen using a mortar and pestle. The powder was added to pre-warmed (65°C) extraction buffer at 20 mL/g of yeast and shaken vigorously. Tubes were subsequently incubated in a 65°C water bath for 10 min and shaken every couple of min. Mixtures were extracted twice with equal volumes chloroform:isoamyl alcohol (24:1) then centrifuged at 3,500 × g for 15 min at 4°C. The aqueous layer was transferred to a new tube and centrifuged at 30,000 × g for 20 min at 4°C to remove any remaining insoluble material. To the supernatant, 0.1 vol 3 M Sodium acetate (pH 5.2) and 0.6 vol isopropanol were added, mixed, and then stored at -80°C for 30 min. Nucleic acid pellets (including any remaining carbohydrates) were collected by centrifugation at 3,500 × g for 30 min at 4°C. The pellet was dissolved in 1 ml TE (pH 7.5) and transferred to a microcentrifuge tube. To selectively precipitate the RNA, 0.3 vol of 8 M LiCl was added and the sample was stored overnight at 4°C. RNA was

pelleted by centrifugation at 20,000 × g for 30 min at 4°C then washed with ice cold 70% EtOH, air dried, and dissolved in 50–150 µl DEPC-treated water.

RNA concentration and 260/280 nm ratios were determined with a NanoDrop ND-1000 spectrophotometer (NanoDrop Technologies, Wilmington, DE, USA), and 1% agarose gels were run to visualize the integrity of the RNA. To improve our ability to visually assess RNA quality, the same RNA samples were run on a TapeStation 4200 system (Agilent Technologies, Santa Clara, CA, USA), using High Sensitivity RNA ScreenTape assays. mRNA isolation was performed using NEBNext Poly(A) mRNA Magnetic Isolation Module (New England Biolabs, Ipswich, MA, USA) and library preparation was achieved using Ion Total RNA-Seq Kit v2 (Thermo Fisher Scientific, Waltham, MA, USA), following manufacturer instructions. Six barcoded samples were simultaneously sequenced on an Ion Proton System (Thermo Fisher Scientific) at the Genome Transcriptome Facility of Bordeaux. Reads are deposited into NCBI SRA database www.ncbi.nlm.nih.gov in the bioproject: PRJNA704978.

4.5. RNA-seq alignment and quantification

For reads alignment, we used a reference genome composed of the sequence of the *S. cerevisiae* laboratory strain S288c (assembly: GCF_000146045.2, www.ebi.ac.uk) manually added with the 34 genes specific of the wine strain EC1118 (assembly: GCA_000218975.1, www.ebi.ac.uk [40]. Alignment was performed using the Torrent Mapping Alignment Program (TMAP) map4 module implemented in the Ion Torrent Suite 5.0.5. Default parameters were used to generate BAM files for each sample.

Galaxy server [41] was used to create tool suites called "workflow" in a simple way: data alignment was checked and filtered using SAMtools [42,43]. Unmapped reads were eliminated, as well as reads with mapping quality <20. The number of reads per gene was counted using HTseq-count [44] with the following options: format (-f) : BAM ; type (-t) : mRNA ; ID (-i) : transcript_id ; Quality min. (-a) : 20. In this case, we use a GFF3 reference file containing features from S288c (EnsemblFungi website, *S. cerevisiae* R64-1-1 release 40) added with the 34 EC1118-specific genes. Finally, gene expression was normalized in Reads Per Kilobase Million [45]. using R software [46]. 6287 genes were quantified.

4.6. RNA-seq statistical analyses

Differentially Expressed Genes (DEG) between wildtype and mutant strains were determined using ANOVA. Levene test was carried out beforehand to verify homoscedasticity. For the genes showing heteroscedasticity, non-parametric tests were performed (Kruskal-Wallis, *agricolae* package, R). The p-values were corrected for multiple tests with the method of Benjamini-Hochberg (FDR, False Discovery Rate). We considered as differentially expressed genes with i- p-values<0.05 and ii- higher than two-fold changes (1124 genes, 22 down-regulated and 1102 up-regulated in the mutant).

For Gene Ontology (GO) analysis, the gene_association.sgd.gz file (December 2003, http://www.geneontology.org/) was used to identify the GO terms associated with all quantified genes. Hypergeometric tests were performed to identify over- or under-represented GO terms (functions, processes or components) for up-regulated and/or down-regulated genes in the mutant. P-values were corrected for multiple tests with the method of Benjamini-Hochberg with R.

Protein-protein interactions were analyzed using STRING database v11 (http://string-db.org/) and the STRINGdb package (R) [47]. For each pair of DEG-genes, a protein-protein interaction (PPI) confidence score was extracted from STRINGdb (http://string-db.org/). Clustering was performed using R *hclust* function and the *complete* method. PPI clusters were defined visually and were retain when i- they contained more than 10 genes and ii- the mean score of the cluster was >0.4. Individual clusters were then explored for specific functions and components using STRING-db.

The enrichment or depletion in histone modification was assessed using data from Pokholok et al, 2005 (http://younglab.wi.mit.edu/nucleosome/DataDownload.html). Briefly, 8 histone modifications (3 acetylations: H3K9ac, H3K14ac and H4ac and 5 methylations: H3K4me1, H3K4me2, H3K4me3, H3K36me3, H3K7me3) were searched in up- or down-regulated genes in the mutant, as well as in non-significant genes between mutant and wildtype. The average ratios of acetylation and methylation in up- and down-regulated genes was compared to those of non-significant genes (Kruskal-Wallis tests, p-value<0.05). P-values were corrected for multiple testing with Benjamin-Hochberg adjustment. The fold enrichment in up- or down regulated genes compared to non-significant ones was also calculated.

4.7. Chemical analyses

4.7.1. Apolars esters analysis

In order to prevent the evolution of ester content, all the wines were then frozen at -20°C until their analysis. Preliminary test confirmed that freezing does not significantly affect the concentration of the investigated compounds (data not shown). Volatiles compounds produced during fermentation in each condition were quantified. The concentrations of 14 esters (Table 1) (6 Fatty Acid Ethyl Esters, 4 Higher Alcohol Acetates and 4 Alkylated Ethyl Esters) in each wine was determined using a head space solid phase microextraction (HS-SPME) followed by gas chromatography–mass spectrometry (GC–MS) as previously described [21].

4.7.2. Quantification of volatile acids and hydroxylated esters by liquid-liquid extraction and GC/MS analysis.

Two hydroxylated esters ethyl 3-hydroxybutanoate (3hC4C2), and ethyl 2-hydroxy-4-methylpentanoate or ethyl-leucate (2h4mC5C2) were assayed according to the method previously described [20]. The same method was also used for quantifying 4 volatile linear acids (C3 to C8) as well as 3 alkylated acids (2mC3, 2mC4 and 3mC4). Monitored ions are listed in Table S7. Compounds were characterized by comparing their linear retention indices and mass spectra with those of standards.

4.7.3. Quantification of Hydroxylated Acids

Concentrations of 3-hydroxy butanoic acid (3hC4) and 2-hydroxy 4-methyl pentanoic acid (2h4mC5) were determined by gas chromatography–mass spectrometry (GC–MS) after derivatization steps as previously described [20].

4.7.4. Higher Alcohol Analyses

Fifty microliters of internal standard (4-methylpentan-2-ol 50 g/L in pure alcohol) were added to a 5 mL wine sample. The solution was homogenized in a vortex shaker, and a microvolume was injected in split mode into an HP-6890 gas chromatograph, coupled to a flame ionization detector (FID) (injector temperature, 200 °C), using a CP-Wax 57 CB column (50 m × 0.32 mm i.d.; film thickness, 0.25 μm; Varian). The oven was programmed at 40 °C for the first minute and raised to 200 °C at 8 °C/min, the final isotherm lasting 20 min. The carrier gas was hydrogen 5.5 (Air Liquide, France)

4.8. Sensory analyses

4.8.1. General conditions.

Sensory analyses were performed as described by Martin and de Revel, (1999). Samples were evaluated at controlled room temperature (20 °C), in individual booths, using covered, black ISO glasses (NF V09-110, 1971) (AFNOR. Sensory analysis − Apparatus − Wine-tasting glass − ISO 3591. Anal. Sensorielle, 1977), containing about 50 mL liquid, coded with three-digit random numbers. Sessions lasted approximately 5 minutes.

 doi:10.20944/preprints202103.0098.v1

4.8.2. Sensory panels.

Panel 1 consisted of 22 judges, 8 males and 14 females, aged 26.4 ± 4.8 (mean±SD). Panel 2 consisted of 17 judges, 6 males and 11 females, aged 27.6 ± 5.3 (mean±SD). All panelists were research laboratory staff at ISVV, Bordeaux University, selected for their experience in assessing fruity aromas in red wines.

4.8.3. Discriminative tests.

Panel 1 were used for the triangular tests of the various aromatic reconstitutions (AR) (Table S4). For these AR, wines fermented with Fx10-AE were supplemented in FAEE, HAA, AEE and HEE up to concentrations found in wines elaborated with commercial yeast Fx10 and wines fermented with Fx10 were supplemented in C3C2 and AEE up to concentrations found in wines elaborated with Fx10-AE in order to have the same esters concentrations in both supplemented wines. These supplemented wines were then compared one to the other (Table S4).

For each triangular test, three numbered samples were presented in random order: two identical and one different. Wines were presented to the panel in duplicate during the same session. Each judge used direct olfaction to identify the sample perceived as different in each test and gave an answer, even if he was not sure. The results of all the triangular tests were statistically analyzed, based on the binomial law corresponding to the distribution of answers in this type of test.

4.8.4. Descriptive testing methods.

First, sensory profiles were realized by panel 2 to precisely describe the nature of the differences observed during the first triangular tests. In a second time, others sensory profiles for the aromatic reconstitutions (Table S4) were evaluated by Panel 1. Wines were presented to the panel in duplicate, during the same session, to evaluate intensities for overall aroma, red-, black-, fresh-, and jammy-fruit characters. These aromatic descriptors were selected as the most typical of red wines from the Bordeaux area [22]. For each sample, the subject rated the intensity of these descriptors on a continuous 10 cm scale printed on paper, labeled "no odor perceived" on the left and "very intense" on the right.

4.9. Statistical analysis

Quantitative data were analyzed using R software using the following tests: tone or wo-way analysis of variance (ANOVA) was applied to a linear model using the *car* package. The conditions of application (*i.e* homogeneity of variance and normality of residuals) were controlled by using Levene's test and Shapiro-Wilk test, respectively. Kruskal-Wallis test were applied using the *agricolae* package allowing the post hoc test based on Fisher's LSD criterium with BH multiple test correction.

5. Conclusions

This functional genetic study allows to reassess the biosynthesis of different classes of esters in the context of the alcoholic fermentation. Beside the four main esterases previously described, we demonstrated the role of two MAGLases (Yju3p and Mgl2p) in the biosynthesis of substituted ethyl esters. The multiple depletion of such esterases has unsuspected consequences on cell viability and on transcriptome regulation by impacting nitrogen and lipid metabolism as well as chromatin modification. The physiological

role of ester biosynthesis has been previously debated. Several authors proposed they detoxify cytoplasm from medium chain fatty acid and/or higher alcohols [8,49] but this hypothesis was never confirmed experimentally. Ester production also play an ecological role by promoting yeast dissemination and migration by attracting insects [50]. In this study, we propose that the biosynthesis of esters could also be involved in acetyl-CoA homeostasis in fermentative conditions.

Supplementary Materials: Table S1: Kinetics parameters, esters and higher alcohols measured in Cabernet Sauvignon grape must, Table S2: Esters and metabolic precursors measured in Merlot and Tempranillo grape, Table S3: Anova table, Table S4. Description of the various aromatic reconstitutions carried out and results obtained after sensory (triangular tests) and statistical analysis, Table S5: Expression fold change of DEG identified. Table S6, primers used, Table S7: Monitored ions for the different compound's quantification. Figure S1: Production level of EASHA of the strains Fx10 (wt), Fx10-ΔAE (*Δatf1, Δatf2, Δeeb1, Δeht1*) and Fx10-ΔME (*Δmgl2, Δeeb1, Δeht1*), Figure S2: Relative contribution of mono-acyl glycerol lipases activities (Mgl2p, Yju3p) on esters and their respective metabolic precursors measured in Merlot and Tempranillo grape must, Figure S3 (File S9): Gene ontology analysis of cellular processes affected in the Fx10-ΔAE mutant.

Author Contributions: Conceptualization, BC, JCB, PM, and WA; strain construction and fermentation, LH, MT, and PM; chemical assay, JCB and MT, RNAseq analysis, RV, SG, and WA; writing—original draft preparation, MT, PM, WA; writing—review and editing, PM, JCB, WA; funding acquisition, JCB, PM. All authors have read and agreed to the published version of the manuscript.

Funding: This research was funded by Pernod Ricard and Biolaffort Companies

Institutional Review Board Statement: Not applicable.

Informed Consent Statement: "Informed consent was obtained from all subjects involved in the study."

Data Availability Statement: All the data.

Acknowledgments: Authors would like to thank Dr Erwan Guichoux for its assistance in RNAseq experiment. The genomic facilities of Bordeaux University Bordeaux received grants from the Conseil Régional d'Aquitaine n°20030304002FA and 20040305003FA, from the European Union FEDER n°2003227 and from Investissements d'Avenir ANR-10-EQPX-16-01)

Conflicts of Interest: PM is employed by the Biolaffort company, MT and BC were employed by Pernod Ricard Company. The funders had no role in the design of the study; in the collection, analyses, or interpretation of data; in the writing of the manuscript, or in the decision to publish the results.

References

1. Sicard, D.; Legras, J.L. Bread, beer and wine: Yeast domestication in the Saccharomyces sensu stricto complex. *Comptes Rendus - Biol.* **2011**, *334*, 229–236, doi:10.1016/j.crvi.2010.12.016.

2. Pisarnitskii, A.F. Formation of Wine Aroma: Tones and Imperfections Caused by Minor Components (Review). *Appl. Biochem. Microbiol.* **2001**, *37*, 552–560, doi:10.1023/A:1012390731145.

3. Collin, S.; Derdelinckx, G.; Dufour, J.-P. Relationships between the chemical composition and sensory evaluation of lager beers. *Food Qual. Prefer.* **1994**, *5*, 145–149, doi:https://doi.org/10.1016/0950-3293(94)90021-3.

4. Gammacurta, M.; Marchand, S.; Albertin, W.; Moine, V.; De Revel, G. Impact of yeast strain on ester levels and fruity aroma persistence during aging of bordeaux red wines. *J. Agric. Food Chem.* **2014**, *62*, 5378–5389, doi:10.1021/jf500707e.

5. Tempère, S.; Marchal, A.; Barbe, J.-C.; Bely, M.; Masneuf-Pomarede, I.; Marullo, P.; Albertin, W. The complexity of wine: clarifying the role of microorganisms. *Appl. Microbiol. Biotechnol.* **2018**, *102*, 3995–4007, doi:10.1007/s00253-018-8914-8.

6. Hirst, M.B.; Richter, C.L. Review of Aroma Formation through Metabolic Pathways of Saccharomyces cerevisiae in Beverage Fermentations. *Am. J. Enol. Vitic.* **2016**, *67*, 361 LP – 370, doi:10.5344/ajev.2016.15098.

7. Sumby, K.M.; Grbin, P.R.; Jiranek, V. Microbial modulation of aromatic esters in wine: Current knowledge and future prospects. *Food Chem.* **2010**, *121*, 1–16, doi:10.1016/j.foodchem.2009.12.004.

8. Saerens, S.M.G.; Delvaux, F.R.; Verstrepen, K.J.; Thevelein, J.M. Production and biological function of volatile esters in Saccharomyces cerevisiae. *Microb. Biotechnol.* **2010**, *3*, 165–177, doi:10.1111/j.1751-7915.2009.00106.x.

9. Hazelwood, L. a; Daran, J.M.; van Maris, a J. a; Pronk, J.T.; Dickinson, J.R. The ehrlich pathway for fusel alcohol production: a century of research on Saccharomyces cerevisiae metabolism (vol 74, pg 2259, 2008). *Appl. Environ. Microbiol.* **2008**, *74*, 3920, doi:10.1128/AEM.00934-08.

10. Yoshioka, K.; Hashimoto, N. Ester Formation by Alcohol Acetyltransferase from Brewers' Yeast. *Agric. Biol. Chem.* **1981**, *45*, 2183–2190, doi:10.1080/00021369.1981.10864861.

11. Mason, a B.; Mason, a B.; Dufour, J.; Dufour, J. Alcohol acetyltransferases and the signi®cance of ester synthesis in yeast. *Yeast* **2000**, 1287–1298.

12. Verstrepen, K.J.; Laere, S.D.M. Van; Vanderhaegen, B.M.P.; Derdelinckx, G.; Dufour, J.; Pretorius, I.S.; Winderickx, J.; Thevelein, J.M.; Delvaux, F.R. Expression Levels of the Yeast Alcohol Acetyltransferase Genes. *Society* **2003**, *69*, 5228–5237, doi:10.1128/AEM.69.9.5228.

13. Minetoki, T.; Bogaki, T.; Iwamatsu, A.; Fujii, T.; Hamachi, M. The purification, properties and internal peptide sequences of alcohol acetyltransferase isolated from Saccharomyces cerevisiae Kyokai No. 7. *Biosci. Biotechnol. Biochem.* **1993**, *57*, 2094–2098.

14. Fukuda, K.; Yamamoto, N.; Kiyokawa, Y.; Yanagiuchi, T.; Wakai, Y.; Kitamoto, K.; Inoue, Y.; Kimura, A. Balance of activities of alcohol acetyltransferase and esterase in Saccharomyces cerevisiae is important for production of isoamyl acetate. *Appl. Environ. Microbiol.* **1998**, *64*, 4076–4078.

15. Kruis, A.J.; Gallone, B.; Jonker, T.; Mars, A.E.; H van Rijswijck, I.M.; M Wolkers-Rooijackers, J.C.; Smid, E.J.; Steensels, J.; Verstrepen, K.J.; M Kengen, S.W.; et al. Contribution of Eat1 and Other Alcohol Acyltransferases to Ester Production in Saccharomyces cerevisiae. **2018**, doi:10.3389/fmicb.2018.03202.

16. Saerens, S.M.G.; Verstrepen, K.J.; Van Laere, S.D.M.; Voet, A.R.D.; Van Dijck, P.; Delvaux, F.R.; Thevelein, J.M. The Saccharomyces cerevisiae EHT1 and EEB1 genes encode novel enzymes with medium-chain fatty acid ethyl ester synthesis and hydrolysis capacity. *J. Biol. Chem.* **2006**, *281*, 4446–4456, doi:10.1074/jbc.M512028200.

17. Knight, M.J.; Bull, I.; Curnow, P. The yeast enzyme Eht1 is an octanoyl-CoA:ethanol acyltransferase that also

functions as a thioesterase. *Yeast* **2014**, 2–5, doi:10.1002/yea.

18. Diaz-Maroto, M.C.; Schneider, R.; Baumes, R. Formation pathways of ethyl esters of branched short-chain fatty acids during wine aging. *J. Agric. Food Chem.* **2005**, *53*, 3503–3509, doi:10.1021/jf048157o.

19. Matheis, K.; Granvogl, M.; Schieberle, P. Quantitation and Enantiomeric Ratios of Aroma Compounds Formed by an Ehrlich Degradation of l-Isoleucine in Fermented Foods. *J. Agric. Food Chem.* **2016**, *64*, 646–652, doi:10.1021/acs.jafc.5b05427.

20. Lytra, G.; Franc, C.; Cameleyre, M.; Barbe, J.-C. Study of Substituted Ester Formation in Red Wine by the Development of a New Method for Quantitative Determination and Enantiomeric Separation of Their Corresponding Acids. *J. Agric. Food Chem.* **2017**, *65*, 5018–5025, doi:10.1021/acs.jafc.7b00979.

21. Antalick, G.; Perello, M.-C.; de Revel, G. Development, validation and application of a specific method for the quantitative determination of wine esters by headspace-solid-phase microextraction-gas chromatography–mass spectrometry. *Food Chem.* **2010**, *121*, 1236–1245, doi:10.1016/j.foodchem.2010.01.011.

22. Pineau, B.; Barbe, J.-C.; Van Leeuwen, C.; Dubourdieu, D. Examples of Perceptive Interactions Involved in Specific "Red-" and "Black-berry" Aromas in Red Wines. *J. Agric. Food Chem.* **2009**, *57*, 3702–3708, doi:10.1021/jf803325v.

23. Lytra, G.; Tempere, S.; Revel, G. de; Barbe, J.-C. Impact of Perceptive Interactions on Red Wine Fruity Aroma. *J. Agric. Food Chem.* **2012**, *60*, 12260–12269, doi:10.1021/jf302918q.

24. Selvaraju, K.; Gowsalya, R.; Vijayakumar, R.; Nachiappan, V. MGL2/YMR210w encodes a monoacylglycerol lipase in Saccharomyces cerevisiae. *FEBS Lett.* **2016**, *590*, 1174–1186, doi:10.1002/1873-3468.12136.

25. Heier, C.; Taschler, U.; Rengachari, S.; Oberer, M.; Wolinski, H.; Natter, K.; Kohlwein, S.D.; Leber, R.; Zimmermann, R. Identification of Yju3p as functional orthologue of mammalian monoglyceride lipase in the yeast Saccharomycescerevisiae. *Biochim. Biophys. Acta* **2010**, *1801*, 1063–1071, doi:10.1016/j.bbalip.2010.06.001.

26. Pokholok, D.K.; Harbison, C.T.; Levine, S.; Cole, M.; Hannett, N.M.; Tong, I.L.; Bell, G.W.; Walker, K.; Rolfe, P.A.; Herbolsheimer, E.; et al. Genome-wide map of nucleosome acetylation and methylation in yeast. *Cell* **2005**, *122*, 517–527, doi:10.1016/j.cell.2005.06.026.

27. Fujii, T.; Nagasawa, N.; Iwamatsu, A.; Bogaki, T.; Tamai, Y.; Hamachi, M. Molecular cloning, sequence analysis, and expression of the yeast alcohol acetyltransferase gene. *Appl. Environ. Microbiol.* **1994**, *60*, 2786–2792, doi:10.1128/aem.60.8.2786-2792.1994.

28. Lilly, M.; Lambrechts, M.G.; Pretorius, I.S. Effect of increased yeast alcohol acetyltransferase activity on flavor profiles of wine and distillates. *Appl. Environ. Microbiol.* **2000**, *66*, 744–753, doi:10.1128/AEM.66.2.744-753.2000.

29. Rollero, S.; Bloem, A.; Camarasa, C.; Sanchez, I.; Ortiz-Julien, A.; Sablayrolles, J.-M.; Dequin, S.; Mouret, J.-R. Combined effects of nutrients and temperature on the production of fermentative aromas by Saccharomyces cerevisiae during wine fermentation. *Appl. Microbiol. Biotechnol.* **2014**, doi:10.1007/s00253-014-6210-9.

30. Seguinot, P.; Bloem, A.; Brial, P.; Meudec, E.; Ortiz-Julien, A.; Camarasa, C. Analysing the impact of the nature of the nitrogen source on the formation of volatile compounds to unravel the aroma metabolism of two non-Saccharomyces strains. *Int. J. Food Microbiol.* **2020**, *316*, doi:10.1016/j.ijfoodmicro.2019.108441.

31. Smit, B.A.; Engels, W.J.M.; Smit, G. Branched chain aldehydes: production and breakdown pathways and relevance for flavour in foods. **2008**, doi:10.1007/s00253-008-1758-x.

32. Lytra, G.; Cameleyre, M.; Tempere, S.; Barbe, J.-C. Distribution and Organoleptic Impact of Ethyl 3-Hydroxybutanoate Enantiomers in Wine. **2015**, doi:10.1021/acs.jafc.5b04332.

33. Galdieri, L.; Zhang, T.; Rogerson, D.; Lleshi, R.; Vancura, A. Protein acetylation and acetyl coenzyme a metabolism in Budding Yeast. *Eukaryot. Cell* **2014**, *13*, 1472–1483, doi:10.1128/EC.00189-14.

34. Marchal, A.; Marullo, P.; Moine, V.; Dubourdieu, D. Influence of yeast macromolecules on sweetness in dry wines: Role of the Saccharomyces cerevisiae protein Hsp12. *J. Agric. Food Chem.* **2011**, *59*, 2004–2010, doi:10.1021/jf103710x.

35. Gietz, R.D.; Schiestl, R.H. High-efficiency yeast transformation using the LiAc/SS carrier DNA/PEG method. *Nat. Protoc.* **2007**, *2*, 31–4, doi:10.1038/nprot.2007.13.

36. Marullo, P.; Bely, M.; Masneuf-Pomarède, I.; Pons, M.; Aigle, M.; Dubourdieu, D.; Masneuf-Pomarede, I.; Pons, M.; Aigle, M.; Dubourdieu, D. Breeding strategies for combining fermentative qualities and reducing off-flavor production in a wine yeast model. *FEMS Yeast Res.* **2006**, *6*, 268–279, doi:10.1111/j.1567-1364.2006.00034.x.

37. Zimmer, A.; Durand, C.; Loira, N.; Durrens, P.; Sherman, D.J.; Marullo, P. QTL dissection of lag phase in wine fermentation reveals a new translocation responsible for Saccharomyces cerevisiae adaptation to sulfite. *PLoS One* **2014**, *9*, 37–39, doi:10.1371/journal.pone.0086298.

38. da Silva, T.; Albertin, W.; Dillmann, C.; Bely, M.; la Guerche, S.; Giraud, C.; Huet, S.; Sicard, D.; Masneuf-Pomarede, I.; de Vienne, D.; et al. Hybridization within Saccharomyces Genus Results in Homoeostasis and Phenotypic Novelty in Winemaking Conditions. *PLoS One* **2015**, *10*, e0123834, doi:10.1371/journal.pone.0123834.

39. Reid, K.E.; Olsson, N.; Schlosser, J.; Peng, F.; Lund, S.T. An optimized grapevine RNA isolation procedure and statistical determination of reference genes for real-time RT-PCR during berry development. *BMC Plant Biol.* **2006**, *6*, 27, doi:10.1186/1471-2229-6-27.

40. Novo, M.; Bigey, F.; Beyne, E.; Galeote, V.; Gavory, F.; Mallet, S.; Cambon, B.; Legras, J.-L.; Wincker, P.; Casaregola, S.; et al. Eukaryote-to-eukaryote gene transfer events revealed by the genome sequence of the wine yeast Saccharomyces cerevisiae EC1118. *Proc. Natl. Acad. Sci.* **2009**, *106*, 16333–16338, doi:10.1073/pnas.0904673106.

41. Goecks, J.; Nekrutenko, A.; Taylor, J.; Team, T.G. Galaxy: a comprehensive approach for supporting accessible, reproducible, and transparent computational research in the life sciences. *Genome Biol.* **2010**, *11*, R86, doi:10.1186/gb-2010-11-8-r86.

42. Li, H.; Handsaker, B.; Wysoker, A.; Fennell, T.; Ruan, J.; Homer, N.; Marth, G.; Abecasis, G.; Durbin, R. The Sequence Alignment/Map format and SAMtools. *Bioinformatics* **2009**, *25*, 2078–2079, doi:10.1093/bioinformatics/btp352.

43. Li, H. A statistical framework for SNP calling, mutation discovery, association mapping and population genetical parameter estimation from sequencing data. *Bioinformatics* **2011**, *27*, 2987–2993, doi:10.1093/bioinformatics/btr509.

44. Anders, S.; Pyl, P.T.; Huber, W. HTSeq--a Python framework to work with high-throughput sequencing data. *Bioinformatics* **2015**, *31*, 166–169, doi:10.1093/bioinformatics/btu638.

45. Mortazavi, A.; Williams, B.A.; McCue, K.; Schaeffer, L.; Wold, B. Mapping and quantifying mammalian transcriptomes by RNA-Seq. *Nat. Methods* **2008**, *5*, 621–628, doi:10.1038/nmeth.1226.

46. R Development Core Team, R. R: A Language and Environment for Statistical Computing. *R Found. Stat. Comput.* 2011, *1*, 409.

47. Franceschini, A.; Szklarczyk, D.; Frankild, S.; Kuhn, M.; Simonovic, M.; Roth, A.; Lin, J.; Minguez, P.; Bork, P.; Von Mering, C.; et al. STRING v9.1: Protein-protein interaction networks, with increased coverage and integration. *Nucleic Acids Res.* **2013**, *41*, doi:10.1093/nar/gks1094.

48. Martin, N.; de Revel, G. Sensory evaluation: scientific bases and oenological applications. *J. Int. des Sci. la Vigne du Vin* **1999**, *33*, 81–93.

49. Malcorps, P.; Cheval, J.M.; Jamil, S.; Dufour, J.-P. A new model for the regulation of ester synthesis by alcohol acetyltransferases in Saccharomyces cerevisiae. *J Am Soc Brew Chem* **1991**, *49*, 47–53.

50. Christiaens, J.F.; Franco, L.M.; Yaksi, E.; Verstrepen, K.J.; Cools, T.L.; De Meester, L.; Michiels, J.; Wenseleers, T.; Hassan, B.A. The Fungal Aroma Gene ATF1 Promotes Dispersal of Yeast Cells through Insect Vectors. *CellReports* **2014**, *9*, 425–432, doi:10.1016/j.celrep.2014.09.009.